

# Dynamin at the Neck of Caveolae Mediates Their Budding to Form Transport Vesicles by GTP-driven Fission from the Plasma Membrane of Endothelium

Phil Oh, Deirdre P. McIntosh, and Jan E. Schnitzer

Department of Pathology, Harvard Medical School, Beth Israel Deaconess Medical Center, Boston, Massachusetts 02215

**Abstract.** The molecular mechanisms mediating cell surface trafficking of caveolae are unknown. Caveolae bud from plasma membranes to form free carrier vesicles through a “pinching off” or fission process requiring cytosol and driven by GTP hydrolysis (Schnitzer, J.E., P. Oh, and D.P. McIntosh. 1996. *Science*. 274:239–242). Here, we use several independent techniques and functional assays ranging from cell-free to intact cell systems to establish a function for dynamin in the formation of transport vesicles from the endothelial cell plasma membrane by mediating fission at the neck of caveolae. This caveolar fission requires interaction with cytosolic dynamin as well as its hydrolysis of GTP. Expression of dynamin in cytosol as well as purified recombinant dynamin alone supports GTP-induced caveolar fission in

a cell-free assay whereas its removal from cytosol or the addition to the cytosol of specific antibodies for dynamin inhibits this fission. Overexpression of mutant dynamin lacking normal GTPase activity not only inhibits GTP-induced fission and budding of caveolae but also prevents caveolae-mediated internalization of cholera toxin B chain in intact and permeabilized endothelial cells. Analysis of endothelium in vivo by subcellular fractionation and immunomicroscopy shows that dynamin is concentrated on caveolae, primarily at the expected site of action, their necks. Thus, through its ability to oligomerize, dynamin appears to form a structural collar around the neck of caveolae that hydrolyzes GTP to mediate internalization via the fission of caveolae from the plasma membrane to form free transport vesicles.

**C**ELLS use vesicular carriers to transport select molecules vectorially from donor to acceptor membrane compartments. Although clathrin-coated vesicles have been the most extensively studied, there are various other clathrin-independent plasmalemmal vesicles that may also function in the trafficking of molecules at cell surfaces. Caveolae are one distinctive type of non-clathrin-coated plasmalemmal vesicle. They are specialized microdomains (Schnitzer et al., 1995c) that appear by electron microscopy to exist as smooth, small (60–80 nm), flask-shaped invaginations located on the surface of many cell types and seem to form through the oligomerization of a structural coat protein called caveolin (Rothberg et al., 1992; Fra et al., 1995; Monier et al., 1995; Sargiacomo et al., 1995).

Upon the discovery of their abundance in endothelium by electron microscopy, a role for caveolae as fluid phase vesicular carriers in the transvascular transport of circulating blood molecules was postulated 40 years ago (Palade, 1958). More recent work suggests that caveolae mediate not only fluid phase but also receptor-mediated endocytosis or transcytosis of molecules (for reviews see Schnitzer, 1993, 1997). Caveolae appear to act as specific vesicular transporters for select blood-borne macromolecules (Milici et al., 1987; Schnitzer and Oh, 1994; Schnitzer et al., 1994; Schnitzer et al., 1995a), conformationally modified proteins (Ghitescu et al., 1986; Schnitzer and Bravo, 1993; Schnitzer et al., 1994), toxins (Montesano et al., 1982; Parton, 1994; Schnitzer et al., 1996), and viruses (Kartenback et al., 1989). Caveolae purified from endothelium in rat lung tissue contain specific binding and transport proteins (for review see Schnitzer, 1997), as well as key signaling molecules (Liu et al., 1997), some of which may interact directly with caveolin (Li et al., 1996). Caveolae also may function as organized signal transduction centers in various cell types (Anderson, 1993; Lisanti et al., 1994; Liu et al., 1997). At least in endothelium they may not only permit the efficient propagation of sensory stimuli at the cell surface but also integrate signaling with vesicular trans-

Address all correspondence to Dr. Jan E. Schnitzer, BIDMC/Research North, Dept. of Pathology, 330 Brookline Ave., Boston, MA 02215. Tel.: (617) 667-3577. Fax: (617) 667-3591. E-mail: jschnitz@bidmc.harvard.edu

This work (except for the immunogold EM and transfection studies) was presented at the American Society for Cell Biology (ASCB) meeting in San Francisco, CA, on December 14–18, 1996, and at the ASCB meeting (including the immunogold EM and transfection studies) in Washington, DC, on December 13–17, 1997, and has appeared in abstract form (Oh, P., and J.E. Schnitzer. 1996. *Mol. Biol. Cell*. 7:83a; Oh, P., D.P. McIntosh, J.E. Schnitzer. 1997. *Mol. Biol. Cell*. 8:425a, respectively).

port (Schnitzer et al., 1995c, 1996; Liu et al., 1997). Disassembly of caveolae in endothelium not only prevents endocytosis or transcytosis of select ligands, which disrupts normal capillary permeability in situ (Schnitzer et al., 1994), but also effectively prohibits regionalized signal and mechano-transduction and the efficient propagation of sensory stimuli at the cell surface (Liu et al., 1997; Schnitzer, 1997). Targeting caveolae in vivo may prove useful in selectively overcoming the endothelial cell barrier for tissue-specific drug and gene delivery (Schnitzer, 1997).

The molecular mechanisms mediating and regulating caveolar trafficking at the cell surface are largely unknown. Caveolae purified from endothelial cell plasma membranes by physical disruption (Schnitzer et al., 1995b,c) and after GTP-induced fission (Schnitzer et al., 1996) contain the molecular transport machinery apparently necessary for regulated, receptor-mediated endocytosis or transcytosis of select ligands via vesicle budding, docking, and fusion (Schnitzer et al., 1995a). Consistent with the existence in caveolae of several molecules ascribed functions in the docking and fusion of ER/Golgi trafficking vesicles as well as synaptic vesicles, both caveolae-mediated endocytosis and transcytosis of macromolecules in endothelium are inhibited by *N*-ethylmaleimide, which inactivates a key vesicle fusion factor called *N*-ethylmaleimide-sensitive fusion protein (Schnitzer et al., 1995a).

Currently even less is known about the budding of caveolae. Until recently it has not even been clear whether caveolae are dynamic vesicular carriers or just static invaginations or "caves" (Schnitzer et al., 1996). Using a permeabilized cultured endothelial cell system and an in vitro-reconstituted, cell-free assay developed for examining the budding, and more precisely, the "pinching off" or fission of caveolae directly from plasma membranes, we have shown that caveolae can indeed bud to form free discrete carrier vesicles through a fission process requiring the presence of cytosol and GTP (Schnitzer et al., 1996). GTP binding without hydrolysis, as assessed by GTP $\gamma$ S, does not permit caveolar fission, and in fact actually prevents it. The internalization of cholera toxin B chain by caveolae is stimulated in endothelial cells by GTP and is almost completely inhibited by GTP $\gamma$ S (Schnitzer et al., 1996). Therefore, it is likely that a cytosolic protein capable of binding and hydrolyzing GTP, namely a GTPase, is associated at least transiently with caveolae and necessary for their fission and internalization to occur.

Here, we identify dynamin as the cytosolic guanine nucleotide-binding protein that mediates the fission and internalization of caveolae in endothelium. We find that cytosolic GTPase-active dynamin is critical for the fission and budding of caveolae whereas mutant dynamins unable to hydrolyze GTP normally are inhibitory. For the first time, dynamin has been localized to its expected site of action, in this case concentrated in caveolae at their necks, where upon its hydrolysis of GTP, it appears to directly mediate vesicular fission from the plasma membrane and thus the internalization of caveolae.

## Materials and Methods

Antibodies to the following antigens were acquired from the following vendors: dynamin (monoclonal) from Transduction Laboratories (Lexing-

ton, KY) or Upstate Biotechnology Inc. (Lake Placid, NY) (HUDY-1) (Transduction Laboratories' antibody was used unless otherwise indicated), and folate receptor (MOV19, monoclonal) from Centocor Inc. (Malvern, PA). Purified recombinant wild-type and K44A dynamins and the ACE antibody were gifts from Drs. S. Schmid (Scripps Research Institute, La Jolla, CA) and R.A. Skidgel (University of Illinois College of Medicine at Chicago, Chicago, IL), respectively. Reagents and other supplies were obtained from the following sources: geneticin (G418) and penicillin-streptomycin solution from Gibco Laboratories (Grand Island, NY); colloidal gold from Electron Microscopy Sciences (Fort Washington, PA); tetracycline, puromycin, fish skin gelatin, and cholera toxin B chain (CT-B)<sup>1</sup> conjugated to FITC (CT-B-FITC) from Sigma Chemical Co. (St. Louis, MO); and DOTAP liposomal transfection reagent from Boehringer Mannheim Corp. (Indianapolis, IN). All other reagents/supplies were obtained as in our past work (Schnitzer et al., 1994, 1995b,c,d, 1996).

## Cell Culture

Bovine lung microvascular endothelial cells (BLMVEC) and bovine aortic endothelial cells (BAEC) were grown as described previously (Schnitzer and Bravo, 1993; Schnitzer et al., 1994, 1995a; Schnitzer and Oh, 1994). As in Damke et al. (1995b), HeLa cells, transfected with either wild-type or K44A (element 1 mutant) dynamin (from Dr. S. Schmid), were grown and induced to express dynamin by removing tetracycline for 48 h before harvesting to isolate cytosol as in Schnitzer et al. (1996).

## Purification of Endothelial Plasma Membranes and Caveolae from Rat Lung

As in Schnitzer et al. (1995c), luminal endothelial cell plasma membranes and caveolae were purified directly from rat lung tissue using an in situ silica-coating procedure. Briefly, the rat lungs were perfused via the pulmonary artery with a colloidal silica solution to coat the luminal surface of the endothelium and allow: (a) selective isolation of the silica-coated endothelial cell plasma membranes (P) from the lung homogenate by centrifugation, and (b) separation and purification of the caveolae (V) from P by shearing and sucrose density centrifugation. The silica-coated membranes stripped of caveolae (P-V) were also collected.

## Immunoaffinity Isolation of Intact Caveolae

Magnetic immunoisolations were performed as in (Schnitzer et al., 1995b; Liu et al., 1997). Briefly, DynaBeads conjugated with anti-mouse IgG were incubated for 5–12 h with monoclonal antibodies against dynamin ( $2 \times 10^8$  beads per 10  $\mu$ g IgG), and then washed by resuspension and magnetic separation. Purified caveolae were incubated at 4°C with these beads overnight before washing and magnetic separation to isolate two fractions: material bound to the beads versus material not bound to the beads.

## Western and Protein Analysis

Proteins of cells and tissue fractions were assessed and quantified by Western analysis as in (Schnitzer et al., 1995b). They were separated by SDS-PAGE (5–15% gels) and electrotransferred onto nitrocellulose filters for immunoblotting using enhanced chemiluminescence autoradiography, followed by densitometric quantification using ImageQuant. Sample protein concentrations were measured using the micro-bincinchoninic acid (BCA) method with BSA as a standard.

## Cell-free Fission Assay

An in vitro-reconstituted, cell-free assay for the fission of caveolae directly from purified plasma membranes was performed as in Schnitzer et al. (1996). Briefly, purified silica-coated endothelial cell plasma membranes, P, were mixed for 60 min at 37°C with ATP and its regeneration system, GTP (1 mM unless indicated otherwise), and filtered cytosol derived from either rat lungs (5.0 mg/ml unless indicated otherwise) as in Schnitzer et al. (1996) or similarly from HeLa cells induced to overexpress either wild-type or K44A dynamin (0.5 mg/ml unless otherwise noted). Ice-cold 60% sucrose was added to make a final concentration of 30% sucrose before

1. *Abbreviations used in this paper:* BAEC, bovine aortic endothelial cells; BLMVEC, bovine lung microvascular endothelial cells; CT-B, cholera toxin B-chain; 5'NT, 5'-nucleotidase; P, plasma membranes; V and V<sub>bud</sub>, purified sheared-off caveolae and GTP-budded caveolae.

adding 5% sucrose to top off the centrifuge tube. This mixture was subjected to centrifugation to sediment the plasma membrane into a pellet well separated from the released floating caveolae (Schnitzer et al., 1996). The pellet proteins were subjected to Western analysis (loading each gel lane with either all of the solubilized material or equal volume fractions) using caveolin antibodies to measure the presence of caveolae and antibodies to noncaveolar plasmalemmal proteins such as  $\beta$ -actin and ACE to assess the general specificity of the effect as well as control for possible variance in the P aliquots and gel loading. During the course of these experiments, we detected  $\beta$ -actin not only in P but also in the cytosols, which in retrospect is not surprising based on its dynamic cytoskeletal function. Therefore, ACE was a better control marker. In some experiments, the budded free caveolae were isolated after centrifugation either at the 5–30% interface or on a continuous sucrose gradient as in Schnitzer et al. (1996).

### Immunodepletion of Dynamin from Cytosol

To immunodeplete dynamin in induced wild-type or K44A dynamin cytosol, 1 ml of filtered cytosol (1 mg/ml) was incubated in the presence of anti-dynamin IgG (3  $\mu$ g) bound to Dynabeads M-450 ( $6 \times 10^7$  beads). The supernatant (immunodepleted cytosol) was removed and checked for the presence of dynamin. The immunodepletion step was repeated (usually once) until no dynamin was detected in the cytosol by immunoblotting.

### Transfection of BLMVEC

5  $\mu$ g wild-type or K44E mutant dynamin-1 full-length DNA subcloned into pSVL (a gift from Dr. R. Vallee, Worcester Foundation for Biomedical Research, Shrewsbury, MA) (Herskovits et al., 1993) was brought to 100  $\mu$ l with DME and mixed for 30 min at room temperature with 100  $\mu$ l of 50% DOTAP liposomal transfection reagent in DME supplemented with 10% FCS. This mixture was brought to 2 ml with DME supplemented with 5% FCS, and added overnight to 40% confluent BLMVEC. After removing this media and incubating for 48 h with DME with 20% FCS, the cells were seeded onto coverslips at 50–60% confluency and incubated in DME with 20% FCS for 48–72 h before the internalization experiments (see below). To assess transfection efficiency, cells overexpressing dynamin were detected by immunofluorescence microscopy using the HUDY-1 antibody. In these experiments, the cells were fixed with 4% paraformaldehyde in PBS for 60 min at room temperature, and then permeabilized with saponin (100  $\mu$ g/ml) in PBS for 30 min. This assay was usually performed after the cells were allowed to endocytose CT-B (see below). In three separate experiments, the transfection efficiencies generally ranged from 40 to 60%.

### Internalization of CT-B in Intact and Permeabilized Cells

After washing with ice-cold DME (3 $\times$ ), BLMVEC grown on coverslips were incubated at 4°C for 30 min with CT-B conjugated to FITC (CT-B-FITC) (8  $\mu$ g/ml in 0.5 ml of DME with 1% BSA). After washing with DME (1 $\times$ ), the cells were incubated for 30 min at 37°C with DME supplemented with 20% FCS to allow CT-B-FITC internalization, fixed with 4% paraformaldehyde in PBS for 60 min at room temperature, and then before mounting and viewing by fluorescence microscopy, washed with PBS (3 $\times$ ) and ddH<sub>2</sub>O (1 $\times$ ). Internalization of surface-bound CT-B-FITC after warm-up was also assessed using permeabilized BLMVEC in the presence of exogenous cytosol and GTP as in Schnitzer et al. (1996).

### Immunofluorescence Microscopy

BLMVEC were grown on coverslips before performing dual immunofluorescence microscopy as in Liu et al. (1997). Briefly, the cells were fixed with acetone or methanol (–20°C for 10 min), blocked with 2% goat serum, and then stained with monoclonal antibodies for dynamin (both antibodies gave similar results) and/or rabbit polyclonal antibody against caveolin (1:250 dilution). The reporter IgG was conjugated with Bodipy (anti-rabbit IgG) and either Texas red or rhodamine (anti-mouse IgG). The immunofluorescence signal was visualized and photographed using an Axiophot microscope (Carl Zeiss Inc., Thornwood, NY) or confocal fluorescence microscope (Bio-Rad Laboratories, Hercules, CA).

### Immunogold Electron Microscopy

Rat lungs were perfused in situ as in Schnitzer and Oh (1994) with two

steps: (1) 30 ml of PBS at 37°C supplemented with 14 mM glucose and 10 mg/ml BSA, and then (2) 4% paraformaldehyde plus 0.5% glutaraldehyde in 0.1 M Na cacodylate-HCl buffer, pH 7.4. Small pieces of lung were cut, immersed in the same fixative for 2 h before washing in 0.2 M Na cacodylate-HCl buffer, infiltrated for 1–2 h with 25% polyvinylpyrrolidone (PVP) containing 2.3 M sucrose in 0.1 M phosphate buffer, pH 7.4, and then mounted on metal nails before freezing in liquid nitrogen. For the in vitro studies, BAEC were fixed in 3% paraformaldehyde for 10 min at room temperature, scraped into Eppendorf tubes, and then pelleted before infiltration with PVP/sucrose as described above.

Thin frozen sections were cut on a Reichert FCS cryoultramicrotome using tungsten-coated glass knives at –100°C. Sections were picked up in 2.3 M sucrose, transferred to Formvar-carbon-coated copper grids, and then floated on PBS before performing immunogold labeling at room temperature as described in Griffiths (1993). Briefly, the grids were floated on drops of 0.5% cold water fish skin gelatin (FSG) for 10 min and incubated for 45 min with 4  $\mu$ g/ml of either the dynamin antibody (HUDY-1 worked better than the other) or another IgG<sub>1</sub> control monoclonal antibody TX4.1934, both diluted in 0.5% FSG. After washing in four drops of PBS for a total of 15 min, the grids were incubated for 20 min with the reporter antibody (goat anti-mouse IgG conjugated to 15- or 5-nm colloidal gold at 1  $\mu$ g/ml), and then washed in four drops of PBS for 15 min and in six drops of ddH<sub>2</sub>O for 20 min. Contrasting/embedding of the labeled grids was carried out on ice in 0.3% uranyl acetate in 2% methyl cellulose for 10 min. Excess liquid was removed by streaking on filter paper leaving a thin coat of methyl cellulose before drying and examination in an electron microscope (100CX; JEOL USA Inc., Peabody, MA). Images were recorded at a primary magnification of 20,000–50,000 $\times$ .

## Results

### Dynamin Antibody Inhibition of GTP-dependent Caveolar Fission

Using an in vitro-reconstituted cell-free system (Schnitzer et al., 1996), we found (as shown in Fig. 1) that antibodies specific for dynamin inhibited the GTP-induced fission of caveolae directly from purified plasma membranes. In this assay, antibody to caveolin was used to quantify the release of caveolae from the endothelial cell plasma membranes by assessing the loss of caveolin. Similar to our past results (Schnitzer et al., 1996), GTP in the presence of ATP and cytosol stimulated fission of caveolae consistently with 70–90% of the caveolae being released. This budding was inhibited in a dose-dependent manner by the presence of anti-dynamin but not control IgG. Comparative densitometry revealed a maximal inhibitory effect of up to 68% with 1–3  $\mu$ g/ml of anti-dynamin IgG. At 3  $\mu$ g/ml, the loss of caveolin signal from the plasma membranes was limited to only 24–31%, which was equivalent to that induced by GTP in the absence of cytosol (data not shown); this suggests that the molecules required for fission are present already on the plasma membrane but at incomplete levels. This antibody appeared to be quite specific for dynamin as assessed by Western analysis of the components used in our budding assays, namely the purified endothelial cell plasma membranes (P) and various cytosols (Fig. 2). Thus, the specific interaction of the antibody with dynamin appeared to inhibit GTP-stimulated fission of caveolae from the plasma membranes.

### GTP-induced Caveolar Fission Enhanced by Dynamin Overexpression

We replaced the rat lung cytosol normally used in our fission assay with cytosol derived from stably transfected HeLa cells induced to express either wild-type or GTPase-

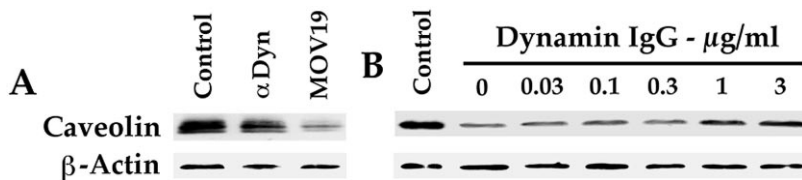


Figure 1. Anti-dynamin IgG inhibits GTP-induced fission of caveolae from endothelial cell plasma membranes. The cell-free assay reconstituting GTP-dependent caveolar fission was performed on purified, silica-coated endothelial cell plasma membranes under standard conditions with GTP (100  $\mu$ M) and rat lung cytosol (1 mg/ml) supplemented with anti-dynamin IgG (0–3  $\mu$ g/ml). Neither GTP nor IgG was added to the samples labeled control. After 1 h, the silica-coated plasma membranes were sedimented by centrifugation and the loss of caveolae was assessed by subjecting all of the membrane pellet to SDS-PAGE and Western analysis using antibodies for caveolin and  $\beta$ -actin. The similar  $\beta$ -actin signal detected in each lane is consistent with the equal aliquots used in the assay and loaded onto the gel lanes. (A) The effect of anti-dynamin IgG was compared with a control IgG (MOV19) (both IgG<sub>1</sub> and at 3  $\mu$ g/ml). (B) The effect of the indicated concentrations of anti-dynamin IgG was assessed. Results shown in A and B are representative of  $\geq 2$  experiments.

deficient K44A mutant dynamin as reported (Damke et al., 1995b). Fig. 3 A shows that the cytosol from the cells induced to express wild-type dynamin was able to support significant fission of caveolae from plasma membranes. Much less budding was detected with the uninduced cytosols and even less with the K44A dynamin-induced cytosol. Immunoblotting of the cytosols revealed greater expression of both the dynamins upon induction (Fig. 3 B). It appeared that the induction was two- to threefold greater in the K44A than in wild-type cytosol. Thus, the expression of wild-type but not K44A dynamin permitted GTP-induced caveolar fission.

#### Effects of Cytosol and GTP on Caveolar Fission from Plasma Membranes

Dynamin overexpression reduced the cytosol requirement but not the GTP concentration necessary for inducing caveolar fission from the purified endothelial cell plasma membranes. In agreement with our past findings (Schnitzer et al., 1996), Fig. 4 A shows that GTP-induced caveolar fission required cytosol and depended on the concentration of cytosol used in the cell-free assay. Western analysis revealed that the ability of GTP to reduce the caveolin signal in the plasma membranes was very dependent on the cytosol concentration. In contrast, the signal for the noncaveo-

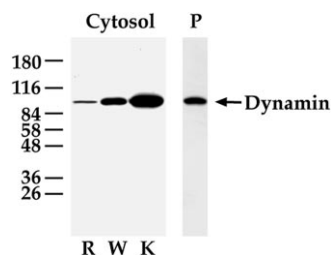


Figure 2. Monospecific immunodetection of dynamin in endothelial cell plasma membranes and various cytosols used in the cell-free assays. Western blot analysis with the monoclonal antibody for dynamin was performed on proteins (10  $\mu$ g) of the silica-coated endothelial cell plasma membranes

purified from rat lungs (P) as well as cytosols derived from either rat lungs (R) or HeLa cells induced to express wild-type dynamin (W) or K44A dynamin (K). Note that by densitometry, the K44A cytosol appeared to have  $\sim 3$ - and 10-fold more dynamin than the wild-type and rat lung cytosols, respectively (of course, assuming equivalent recognition by the antibody). It also should be noted that the other dynamin antibody (HUDY-1) also was quite specific with a single reactive band detected strongly in P (data not shown).

lar plasmalemmal marker protein ACE did not decrease. Both rat lung and wild-type cytosols supported fission but the latter was much more effective at lower concentrations. Fig. 4 B shows that when we quantified the caveolin signal densitometrically and plotted it as a function of the cytosol concentration, the dose response curves were quite distinct with the curve for wild-type cytosol shifted about one order of magnitude more to the left of the rat lung cytosol curve. Maximal caveolar fission was observed with an  $\sim 80\%$  decrease in caveolin signal when the membranes were treated with 0.5 or 5 mg/ml of wild-type cytosol or rat lung cytosol, respectively. The wild-type cytosol was effective at concentrations as low as 0.05 mg/ml, whereas the rat lung cytosol required at least 0.5 mg/ml. The apparently greater expression of dynamin in the wild-type cytosol (Fig. 2) might reduce the required cytosol concentration. As quantified in Fig. 4 B, caveolar fission was not detected in the presence of the K44A cytosol.

Another way to examine the fission of caveolae from the plasma membranes is to isolate the GTP-induced, budded caveolae by flotation as in Schnitzer et al. (1996). Fig. 4, C and D show that both the amount of caveolin released from P and then concurrently recovered in the floating budded caveolae ( $V_{\text{bud}}$ ) was dependent on wild-type cytosol concentration. Without cytosol or at low concentrations, a minimal level of budding was detected either at the plasma membrane or in the low density fraction. Starting at 10  $\mu$ g/ml, we found more caveolin was released from P with a concurrent increase in caveolin signal in  $V_{\text{bud}}$ . The

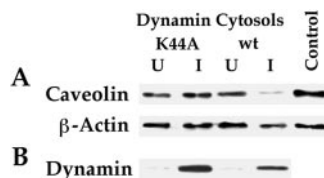
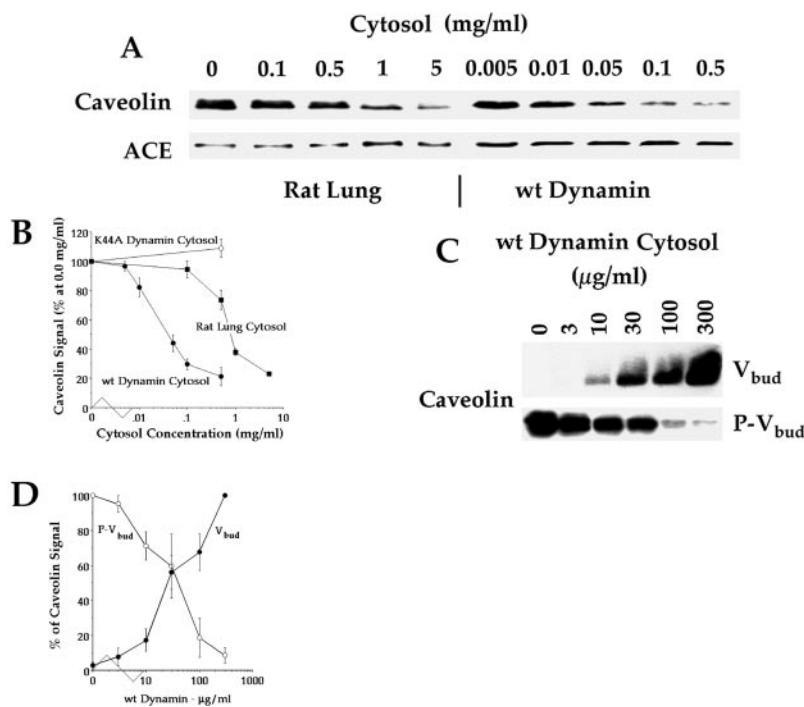


Figure 3. Cytosol from cells induced to express wild-type (but not K44A) dynamin supports GTP-dependent caveolar fission. The standard cell-free caveolar fission assay was performed on P with Western analysis for caveolin

and  $\beta$ -actin as shown. (A) This assay was performed in the presence of buffer without cytosol (Control) or with the indicated cytosols (30  $\mu$ g/ml) isolated from HeLa cells either uninduced (U) or induced (I) to express either wild-type dynamin or the K44A mutant dynamin. (B) Western analysis of dynamin levels in the induced and uninduced cytosols (10  $\mu$ g of protein per lane). Results shown in A and B are representative of at least two experiments.



**Figure 4.** Effect of cytosol concentration and dynamin overexpression on GTP-induced caveolar fission. The standard cell-free caveolar fission assay was performed on P in the presence of indicated cytosols at the indicated concentrations. (A) Western analysis for caveolin and ACE using the repelleted membranes after treatment. (B) Caveolin signal, which is plotted as a function of cytosol concentration was quantified densitometrically and expressed as the percentage of the signal detected in the absence of cytosol. Each point gives the average value with SD from three experiments, one of which is shown in A. (C) Western analysis for the indicated proteins on both the isolated budded caveolae ( $V_{bud}$ ) and the repelleted plasma membranes ( $P-V_{bud}$ ) after budding in the presence of the indicated concentration of wild-type dynamin cytosol. (D) Caveolin signal quantified in  $P-V_{bud}$  (●) and  $V_{bud}$  (○) as a function of wild-type dynamin cytosol concentration. The densitometric signal is expressed as a percentage of the maximum detected signal: for  $P-V_{bud}$  that is in the absence of cytosol and for  $V_{bud}$  that is at the highest concentration of cytosol used (300  $\mu$ g/ml). Each point with SD represents the average of three experiments of which one is shown in C.

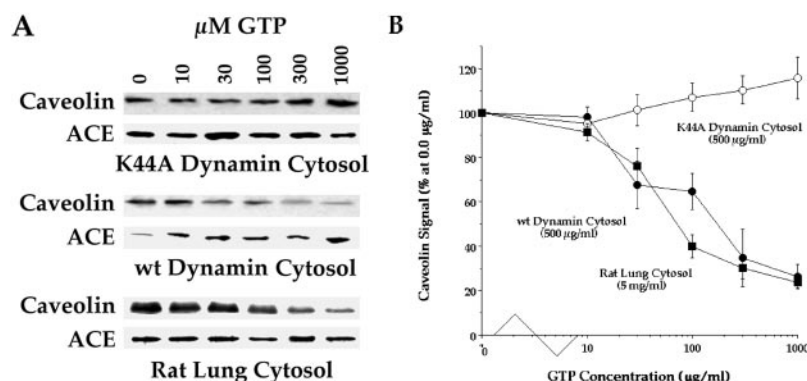
budding detected in each compartment increased to an apparent maximum at 100–300  $\mu$ g/ml. Note that caveolin was not detected by Western analysis in the cytosol nor the whole HeLa cell lysates (data not shown).

Fig. 5 A shows the effects of GTP concentration on caveolar fission in the presence of the different cytosols. Rat lung and wild-type, but not K44A, cytosol supported caveolar fission in a GTP-dependent manner. The caveolin signal decreased in P treated with wild-type cytosol whereas ACE and  $\beta$ -actin did not. As quantified in Fig. 5 B, the GTP dose response curves for caveolar fission were nearly identical for both rat lung and wild-type cytosol with an effective dose to achieve half maximal response ( $ED_{50}$ ) of  $\sim$ 30  $\mu$ M GTP. Conversely, with K44A cytosol, even the highest GTP levels were ineffective. This mutant dynamin is known to lack normal GTPase activity because of a mutation in its GTP binding domain caused by replacing lysine-44 with alanine (Damke et al., 1994). In the presence of the rat lung or wild-type cytosols, GTP $\gamma$ S was unable to stimulate caveolar fission and in fact was quite in-

hibitory (data not shown) which agrees with our past work (Schnitzer et al., 1996). Thus, caveolar fission to release free transport vesicles appeared to require GTP hydrolysis by dynamin.

#### Caveolar Budding in Permeabilized Cells Requires GTP Hydrolysis by Dynamin

The results described above were confirmed in a different assay described in (Schnitzer et al., 1996) using cultured BLMVEC that were permeabilized to replace the endogenous cytosol with exogenous filtered cytosol supplemented with GTP and ATP. Caveolar budding was detected by then isolating plasma membranes from these cells to assess caveolin levels. Fig. 6 demonstrates that consistent with past results (Schnitzer et al., 1996), incubation of BLMVEC with GTP (but not GTP $\gamma$ S) stimulated the budding of caveolae. This budding was supported by both rat lung and wild-type cytosols but not the K44A cytosol as detected by a 71, 89, and 0% reduction in caveolin signal, re-



**Figure 5.** GTP dependence of caveolar fission in various cytosols. The standard cell-free caveolar fission assay was performed on P with Western analysis for caveolin, ACE, and  $\beta$ -actin as shown in A. P was incubated with GTP at the indicated concentrations plus the indicated cytosols. Unlike caveolin, the signal for both ACE and  $\beta$ -actin remained unchanged, consistent with the equivalent loading of the treated resedimented P onto each gel lane. (B) The caveolin signal in this assay was quantified as in Fig. 4 and then plotted as function of GTP concentration. Each point gives the average value with SD from three or more experiments.

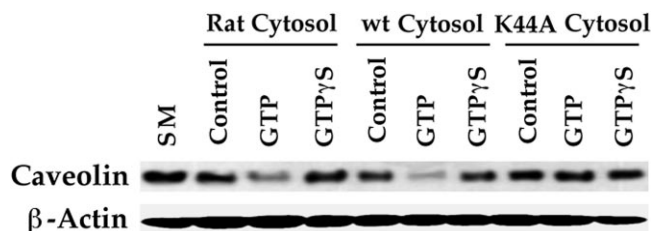


**Figure 6.** Budding of caveolae from the surface of BLMVEC requires GTP hydrolysis and GTPase-competent dynamin. Caveolar budding was assessed in cultured cells as previously described (Schnitzer et al., 1996). Briefly, BLMVEC were permeabilized with streptolysin O, incubated for 10 min at 37°C with the indicated cytosol (rat lung cytosol [1 mg/ml], wild-type or K44A cytosol [0.5 mg/ml]) in cytosolic buffer alone (*Control*) or supplemented with either GTP or GTP $\gamma$ S to a final concentration of 100  $\mu$ M. The BLMVEC plasma membranes were purified for Western analysis using caveolin antibodies to quantify cell surface caveolae and  $\beta$ -actin antibodies as a control. As an additional reference, the plasma membrane was isolated from cells left untreated and not permeabilized (*SM*). Two experiments showed nearly identical results.

spectively. It appeared that budding of caveolae in BLMVEC also required GTP hydrolysis by dynamin.

#### ***GTPase-active Dynamin Is Necessary and Sufficient for GTP-induced Caveolar Fission***

The results described above provided strong evidence for dynamin as a key protein in cytosol required for caveolar fission. To more directly examine our hypothesis that dynamin was the GTPase mediating caveolar fission, we immunodepleted dynamin from the wild-type and K44A cytosols before performing the cell-free fission assay. As shown in Fig. 7 *A*, caveolar fission was easily detected with the wild-type cytosol but not detected after dynamin removal. Fission was rescued, however, when the dynamin-depleted cytosol was replenished with purified recombinant wild-type dynamin but not the K44A mutant. Addition of purified wild-type (but not K44A) dynamin to the dynamin-depleted K44A cytosol created a cytosol able to support GTP-induced caveolar fission. Thus, GTPase-active dynamin was required for this fission process.

Fig. 7 *B* shows that dynamin was also sufficient to permit this fission. In the presence of GTP and ATP, caveolar fission was quite extensive when the cytosol was replaced with purified recombinant wild-type dynamin but not the K44A mutant. It is inappropriate to interpret these results beyond the conditions of the *in vitro* assay to mean that no other molecules play a role in fission. It is very likely that various molecules will at least have a regulatory role in fission through their effects on dynamin (see model proposed in Discussion). A process of activation of dynamin will be necessary to increase its GTPase activity from its moderate baseline level to the critical level required for fission. Of course, this activation hurdle is bypassed in our cell-free assay by providing ample substrate, namely GTP at 0.1–1 mM. Under the conditions of this assay, dynamin was the only protein essential in cytosol for GTP-induced caveolar fission, and required its ability to hydrolyze GTP to be effective.

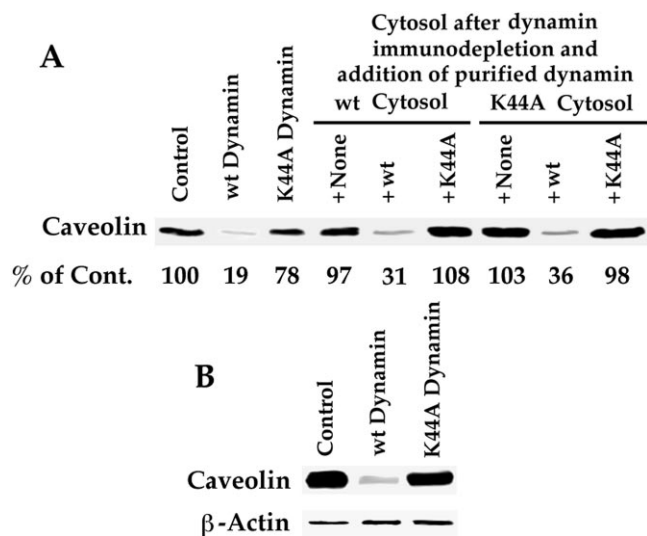


**Figure 7.** GTPase-active dynamin is necessary and sufficient for GTP-induced fission of caveolae. The standard cell-free caveolar fission assay was performed on P with Western analysis for caveolin. (*A*) Requirement for dynamin in cytosol. P was incubated with the indicated cytosols: wild-type or K44A dynamin cytosol, either cytosol immunodepleted of dynamin or either immunodepleted cytosol replenished with purified recombinant wild-type or K44A dynamin. The percentage of caveolin quantified by densitometry and calculated relative to the control is indicated below each lane. (*B*) Dynamin alone can replace cytosol in GTP-induced fission assay. P was incubated with purified recombinant wild-type or K44A dynamin (1  $\mu$ g/ml). Neither dynamin was added to the sample labeled control. The caveolin signal decreased by 73% in the presence of wild-type but not K44A dynamin. The  $\beta$ -actin signal remained constant. Both experiments were performed twice with nearly identical results.

#### ***Mutant Dynamin Inhibits GTP-induced Caveolar Fission***

Having found that dynamin lacking normal GTPase activity does not support caveolar fission, we wondered if this mutant dynamin could actually inhibit caveolar fission. Fig. 8 shows that the addition of K44A dynamin to active wild-type cytosol significantly inhibited GTP-induced caveolar fission. This inhibitory effect was not really surprising because in direct binding assays, K44A and wild-type dynamin bound rather equivalently to the endothelial cell plasma membranes (our unpublished observations). Because this mutant dynamin appeared to interact normally with caveolae, it would be correctly positioned to interfere with the completion of the fission reaction through its inability to hydrolyze GTP.

#### ***Assessing GTP-induced Fission Using Other Caveolar and Plasmalemmal Markers***

For the sake of completeness and to avoid logical concerns attendant to any assay limited to detection by only one probe, we also tested other plasmalemmal and caveolar markers in our reconstituted cell-free system. Although there were several good antibodies specifically recognizing general plasmalemmal markers for the endothelium including ACE,  $\beta$ -actin, and 5'-nucleotidase (5'NT), there simply were not many good antibodies to caveolae-specific

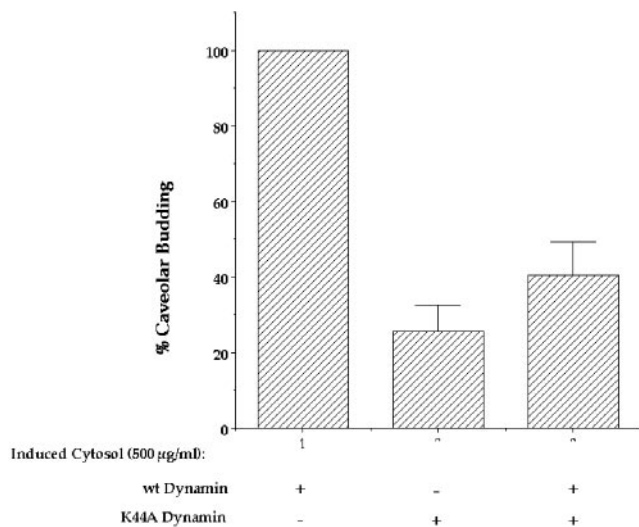


**Figure 8.** K44A mutant dynamin inhibits GTP-induced, dynamin-dependent caveolar fission. The standard cell-free caveolar fission assay was performed on P in the presence of no cytosol, wild-type dynamin cytosol, K44A cytosol, or wild-type and K44A dynamin cytosol combined, each at 500 µg/ml. Budding of caveolae was calculated from the loss of caveolin signal, which was quantified densitometrically. Each value represents the mean of three experiments.

proteins at the time we began these studies. The commercially available antibody for caveolin was the best choice because it is quite specific and caveolin is a structural coat protein of the caveolae (Rothberg et al., 1992). Recently, we made some caveolae-specific monoclonal antibodies and one of these antibodies, TX3.833, especially recognized an 85-kD protein found within caveolae of endothelium only in lung tissue (Schnitzer, 1997). In addition, the sialoglycolipid  $G_{M1}$  is quite enriched in caveolae, and mediates the endocytosis of cholera toxin by caveolae (Montesano et al., 1982; Parton 1994; Schnitzer et al., 1995c, 1996). To examine these additional markers, we performed the cell-free assay using either the wild-type or K44A cytosol. Fig. 9 shows that like caveolin, the plasma-membral signal for  $G_{M1}$  and the TX3.833 antigen was diminished by >80% with the wild-type cytosol relative to the K44A cytosol. Interestingly, the dynamin signal also decreased quite significantly whereas the general plasma-membral markers, 5'NT, ACE, and  $\beta$ -actin, remained quite constant.

#### Mutant Dynamin Prevents Internalization of Caveolae in Cultured Endothelial Cells

Because mutant dynamin lacking normal GTPase activity inhibited caveolar fission in our cell-free assay, then its expression in intact cultured endothelial cells might prevent the internalization of caveolae and their molecular cargo. We previously showed by fluorescence and electron microscopy that cholera toxin B chain (CT-B) is internalized by the caveolae of cultured BLMVEC with accumulation in intracellular multivesicular bodies (Schnitzer et al., 1996). Similar CT-B endocytosis by caveolae was also found in other cell types (Montesano et al., 1982; Parton,

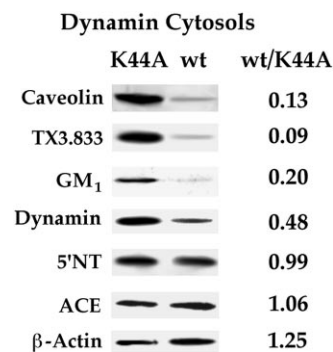


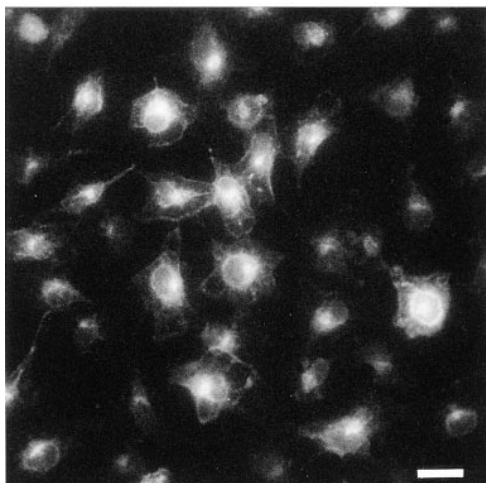
**Figure 9.** GTP in the presence of wild-type but not K44A dynamin depletes the plasma membrane of various caveolar markers but not general plasma-membral proteins. The standard cell-free caveolar fission assay was performed on P in the presence of wild-type dynamin cytosol or K44A dynamin cytosol (each at 500 µg/ml) followed by Western analysis with antibodies to the indicated proteins.

1994). Here, we used CT-B to examine caveolar endocytosis in BLMVEC transfected with the cDNA of wild-type dynamin or the K44E mutant dynamin defective in GTPase activity (Herskovits et al., 1993). Fluorescence microscopy (Fig. 10) indicated that transfection with the mutant dynamin cDNA prevented endocytosis of CT-B-FITC. In this assay, the CT-B-FITC was bound to the cell surface at 4°C before warming the cells to 37°C for 30 min to allow internalization. With wild-type dynamin, ample internalization of CT-B was evident by the extensive perinuclear accumulation of signal in nearly all the cells. Conversely, the inhibitory effect of the GTPase-deficient mutant dynamin was not subtle. It prevented CT-B uptake by the cells with little detectable perinuclear staining (no nuclear ghost image) and ample cell surface staining. Thus, the lack of CT-B accumulation inside these cells did not result from the inhibition of CT-B binding to the cell surface but rather the movement of CT-B from the cell surface into the cell.

Further analysis by counting the cells exhibiting accumulation of intracellular CT-B confirmed the dominant-negative effect of the mutant dynamin. Table I provides a summary of our results. In both the control cells and the cells subjected to transfection with wild-type dynamin cDNA, ~80% of the cells internalized CT-B-FITC readily. For the cells subjected to transfection with the K44E cDNA, the percentage of cells exhibiting CT-B internalization decreased to 35% with about two-thirds of all the cells only showing CT-B staining at the cell surface. In experiments where dynamin immunostaining was performed on the cells after CT-B internalization, nearly all of the cells overexpressing the mutant dynamin showed little to no evidence for CT-B internalization (Table I). When focusing only on the dynamin overexpressors, we found that nearly 90% of the cells overexpressing wild-type dynamin were able to endocytose CT-B significantly as indicated by a strong perinuclear signal causing a readily apparent nuclear "ghost" image. Conversely, CT-B internalization was detected in <10% of the cells expressing the K44E dynamin even though 90% of these cells showed significant cell surface staining with the CT-B-FITC. Thus, caveolae-mediated internalization of CT-B was inhibited greatly by the overexpression of mutant dynamin unable to hydrolyze GTP properly.

Similar results were obtained in experiments examining CT-B-FITC endocytosis by permeabilized BLMVEC incubated with exogenous cytosol and GTP. As summarized

A



B

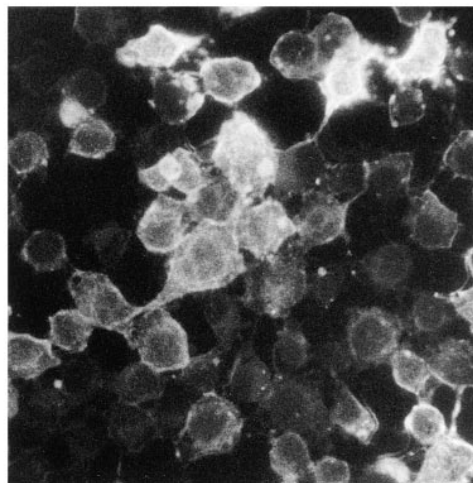


**Figure 10.** Mutant dynamin prevents CT-B internalization in intact cells. BLMVEC were transfected with either wild-type (A) or K44E (B) dynamin cDNA before examining by fluorescence microscopy the internalization of cell surface-bound CT-B-FITC upon warming to 37°C for 30 min. Bar, 5  $\mu$ m.

in Table I, wild-type but not K44A dynamin cytosol from the HeLa cells supported CT-B endocytosis by these permeabilized cells. As reported previously (Schnitzer et al., 1996), GTP stimulated caveolae-mediated CT-B endocytosis, whereas GTP $\gamma$ S inhibited it. When lung cytosol was added to the permeabilized cells with GTP,  $\sim$ 80% of the cells internalized CT-B in 30 min. But without exogenous GTP, intracellular accumulation of CT-B was detected in only about 40% of the cells. When GTP $\gamma$ S replaced GTP, CT-B remained on the cell surface with little evidence of endocytosis (detected in only 10% of the cells). Replacing the lung cytosol with wild-type dynamin cytosol had little effect (79 vs. 85%). Conversely, CT-B internalization was detected in <30% of the cells incubated with K44A cytosol plus GTP. Thus, in both permeabilized cells and trans-

fectured intact cells, the mutant dynamin greatly inhibited the caveolae-mediated endocytosis of CT-B.

#### *Dynamin Enrichment in Purified Plasma Membranes and Caveolae of Endothelium*

Although a functional role for dynamin in caveolar fission and transport was quite apparent, it was necessary to establish where dynamin exists on the endothelial cell surface. First, by subcellular fractionation, we found that dynamin did indeed associate *in vivo* with the endothelial cell plasma membrane rather concentrated in its caveolae. Fig. 11 shows dynamin in caveolin-rich caveolae that, as reported previously (Schnitzer et al., 1995c), were purified to homogeneity from luminal endothelial cell plasma membranes derived directly from rat lung tissue. Dynamin was enriched in the purified silica-coated plasma membranes (P) relative to the starting lung homogenates (H), and was even further enriched 12-fold in the purified caveolae (V) relative to P. Interestingly, we found that the dynamin interaction sites on these membranes were not saturated, probably because of dissociation of dynamin during the dilutional steps of the purification process. In the absence of GTP and GTP $\gamma$ S, the dynamins from the rat lung, wild-type, and K44A cytosols were able to bind the purified membranes quite similarly and tended to reach binding saturation at concentrations found to be optimal for the GTP-induced fission of caveolae (data not shown).

The presence of dynamin and caveolin in the same caveolar vesicles was verified by immunoaffinity isolation performed on V with magnetic beads. Consistent with the previously noted homogeneity of this preparation of caveolae (Schnitzer et al., 1995c), >97% of caveolin in V (Fig. 11 B) and >95% of the proteins found in V were immunoprecipitated with the dynamin antibody. Conversely, in the control, little if any caveolae were bound to the magnetic beads. Dynamin as well as the epitope recognized by the antibody was present and accessible on the outside of nearly all the membrane vesicles found in this caveolae fraction. The lack of membranes in this preparation without dynamin and caveolin is consistent with a putative

**Table I.** Internalization of CT-B-FITC by BLMVEC as Detected by Fluorescence Microscopy

Treatment	Total No. cells	Intracellular CT-B		
		No. of cells	Percent of cells	N
Null	197	155	79 $\pm$ 5	3
Transfection:				
All cells				
Wild-type dynamin cDNA	300	253	83 $\pm$ 3	3
K44E dynamin cDNA	303	103	35 $\pm$ 7	3
Dynamin overexpressors				
Wild-type dynamin cDNA	122	103	87 $\pm$ 4	3
K44E dynamin cDNA	111	10	9 $\pm$ 5	3
Permeabilized cells with GTP:				
Wild-type dynamin cytosol*	300	254	85 $\pm$ 4	3
K44E dynamin cytosol*	290	86	29 $\pm$ 7	3
Permeabilized cells:				
Lung cytosol <sup>‡</sup>	193	79	41 $\pm$ 6	2
GTP and lung cytosol <sup>‡</sup>	230	180	78 $\pm$ 3	2
GTP $\gamma$ S and lung cytosol <sup>‡</sup>	154	15	10 $\pm$ 3	2

*Null*, includes untreated intact cells as well as intact cells processed through the transfection procedure but without the dynamin cDNA. The results were nearly the same so they were combined.

\*30 min warm-up internalization of surface bound CT-B-FITC.

<sup>‡</sup>10 min warm-up internalization of surface bound CT-B-FITC.

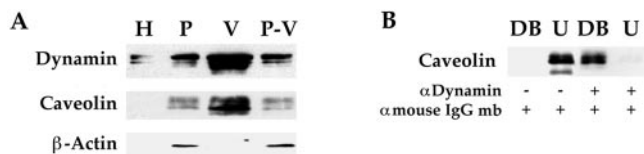


**Figure 11.** Dynamin associated with the endothelial cell plasma membrane *in vivo* concentrates in caveolae. (A) Western analysis with antibodies to dynamin and caveolin was performed on the proteins (5  $\mu$ g) from the following membrane fractions: rat lung homogenate (H), purified silica-coated plasma membranes (P), purified caveolae (V), and plasma membrane stripped of caveolae (P-V). (B) Immunoaffinity isolation of caveolae with dynamin antibody. The purified caveolae (V) were incubated with anti-mouse IgG Dynabeads either alone or prebound with anti-dynamin IgG. The Dynabeads plus any bound material (DB) were separated magnetically from the unbound material (U) before Western analysis of both fractions. Results shown in A and B are representative of at least two experiments.

structural role for dynamin in caveolae (see Discussion) and a minimal level of contamination in V. It appeared that all intact caveolin-coated caveolae purified from the luminal endothelial cell plasma membranes contain dynamin.

#### *Dynamin Colocalization with Cell Surface Caveolin*

Confocal immunofluorescence microscopy was used to assess further the association of dynamin with caveolae. Fig. 12 shows that double immunostaining for dynamin and caveolin in BLMVEC revealed extensive colocalization at the cell surface. Dynamin was easily detected at the cell surface. Dynamin's punctate staining pattern was very similar to, and overlapped significantly but not completely with, that of caveolin. High magnification scans confirm the direct overlap of the signals (Fig. 12, D, E, and F). These findings provide further evidence that dynamin can associate with caveolae, in this case, on the surface of intact cultured endothelial cells under physiological conditions.

#### *Dynamin at the Neck of Endothelial Caveolae In Vivo*

Although it appeared logical that dynamin mediated fission at the neck of the caveolae, to date there was no direct evidence under normal physiological conditions *in vivo* for the existence of dynamin at the neck of caveolae or for that matter any type of budding plasmalemmal vesicle, whether clathrin-coated or not (see Discussion for details). Thus, to affirm a physiological role for dynamin in fission, it seemed imperative that we attempt to localize dynamin in endothelium to its presumed, but so far undemonstrated, site of action. We performed immunogold electron microscopy on ultra-thin cryosections of rat lung tissue that have abundant caveolae in the microvascular endothelium.

As shown in Fig. 13, we detected dynamin specifically on the endothelial cell surface primarily at the neck of caveolae. The dynamin antibody gave ample cell surface labeling whereas little, if any, gold labeling was found with the control antibody (compare Fig. 13, A and F). Morphometric analysis (Table II) revealed that nearly 70% of the

dynamin in endothelium was associated with the plasma membrane, with about two-thirds of the remaining 30% detected in the cytoplasm and one-third (~10%) on other intracellular membranes. More than 50% of all the detected dynamin was in the caveolae (172 of the 330 gold particles counted). Of the gold particles located at the plasma membrane, we found 75% of them associated directly with caveolae, which agrees well with our biochemical and immunofluorescence findings. More importantly, we found 75% of the caveolae-associated gold particles to be located at the caveolar neck.

Caveolae, especially in endothelium *in vivo*, can form racemose invaginations with several vesicles attached to each other in a grape-like cluster of vesicles extending into the cell. It was apparent that some of the gold detected at the caveolar bulb actually might be associated with dynamin present at the neck of two adjoining caveolar vesicles as shown in Fig. 13 B. In some cases, such adjoining caveolar vesicles might not be readily apparent in the plane of the ultra-thin cryosection; this might contribute to some of the gold detected on the plasmalemmal proper where a nearby caveola might not be evident. Because of the great abundance of caveolae in rat lung endothelium, these considerations might account for more than half of the gold detected in these other regions. Even without any correction for these factors, it was quite clear that dynamin under native conditions *in vivo* was located at the endothelial cell surface predominantly around the neck of the caveolae, its expected site of action in caveolar fission.

#### *Lack of Clathrin-coated Vesicles on Rat Lung Microvascular Endothelial Cell Surface In Vivo*

Interestingly, it should be mentioned that during the electron microscopy described above, we detected few, if any, clathrin-coated invaginations on the microvascular endothelial cell surface in the rat lung *in vivo*. This rather surprising finding caused us to explore this issue further by performing Western analysis on the luminal endothelial cell plasma membranes purified from rat lung versus liver tissue (we know from electron microscopy that the latter has endothelial cell surface, clathrin-coated invaginations). As shown in Fig. 14, we did not find the clathrin heavy chain on the luminal endothelial cell plasma membranes purified from rat lung, although it was amply present in the starting homogenate. Conversely, both the liver homogenates and the purified endothelial cell plasma membranes from the liver contained significant levels of clathrin. Clearly in the liver there are many non-endothelial cells known to have an abundance of clathrin-coated vesicles (i.e., hepatocytes and Kupffer cells). It should also be pointed out that when we immunoblotted these preparations for caveolin, the opposite distribution was detected. We found caveolin expressed in the rat lung and especially enriched in the endothelial cell plasma membranes purified from the lung tissue. There was little expression in the liver. Thus, these findings support a scarcity of clathrin-coated invaginations at the cell surface of lung microvascular endothelium as it exists in its native state *in vivo*. Conversely, the liver endothelial cell surface has abundant clathrin-coated vesicles but no apparent caveolae *in vivo*.

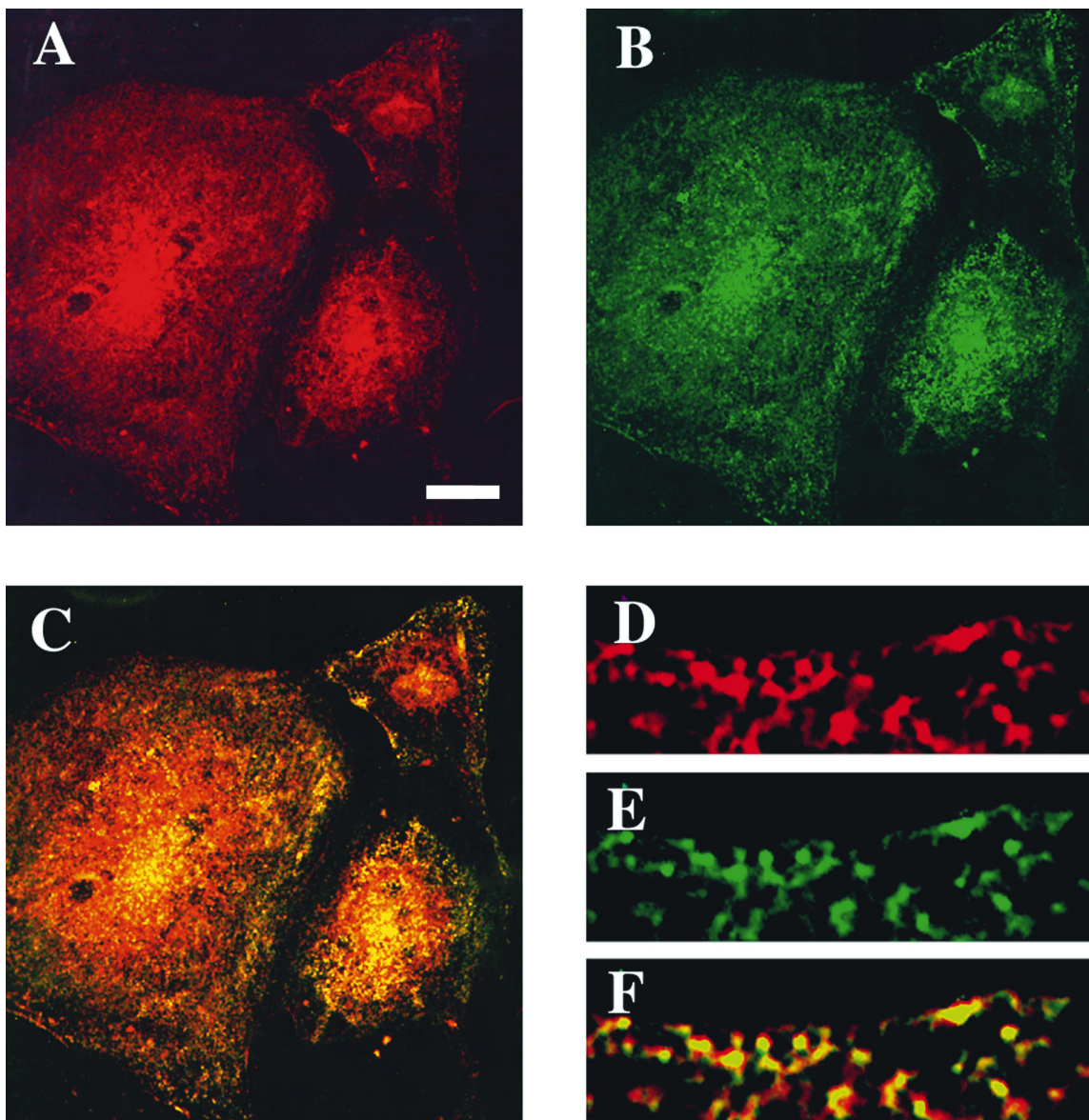


**Figure 12.** Colocalization of caveolin and dynamin at the endothelial cell surface. Immunofluorescence confocal microscopy was performed on BLMVEC using antibodies against dynamin and caveolin. The signals for dynamin (*red*) (A and D) and caveolin (*green*) (B and E) overlap significantly on the cell surface as shown by the orange-yellow signal denoting colocalization in the composite, superimposed image (C and F). Little, if any, staining was detected in the absence of primary antibodies or with other antibodies as negative controls (data not shown). Bar, (A–C) 20  $\mu\text{m}$ ; (D–F) 2  $\mu\text{m}$ .

### ***Dynamin on Caveolae and Clathrin-coated Invaginations in Cultured Endothelial Cells***

Past work shows dynamin labeling of the bulb regions of clathrin coated invaginations in HeLa cells (Damke et al., 1994). These cells do not have detectable expression of caveolin nor morphologically identifiable caveolae by electron microscopy (our unpublished observations). Thus it would be of interest to examine dynamin's distribution in cells that have both types of invaginations. Endothelial cells change phenotypically when isolated and grown in culture (Schnitzer, 1997). They have both caveolae and clathrin-coated vesicles on their cell surface although the density of caveolae is at least 10-fold less *in vitro* than *in vivo*. We took advantage of this to assess the distribution

of dynamin in endothelial cells having both types of vesicles. As shown in Fig. 15, immunogold labeling of BAEC showed the presence of dynamin on clathrin-coated pits and invaginations as well as caveolae. Clathrin-coated pits at different stages of budding were detected. Rather strong dynamin labeling of coated pits was detected. The dynamin was primarily in the bulb region whereas for caveolae it was in the neck region. Thus, dynamin can be present on both types of invaginations in a single cell type.

### ***Free GTP-budded Caveolar Vesicles Carry Caveolar Markers but Release Dynamin***

At the end of our investigation, we decided to perform Western analysis to characterize, at least partially, the mo-

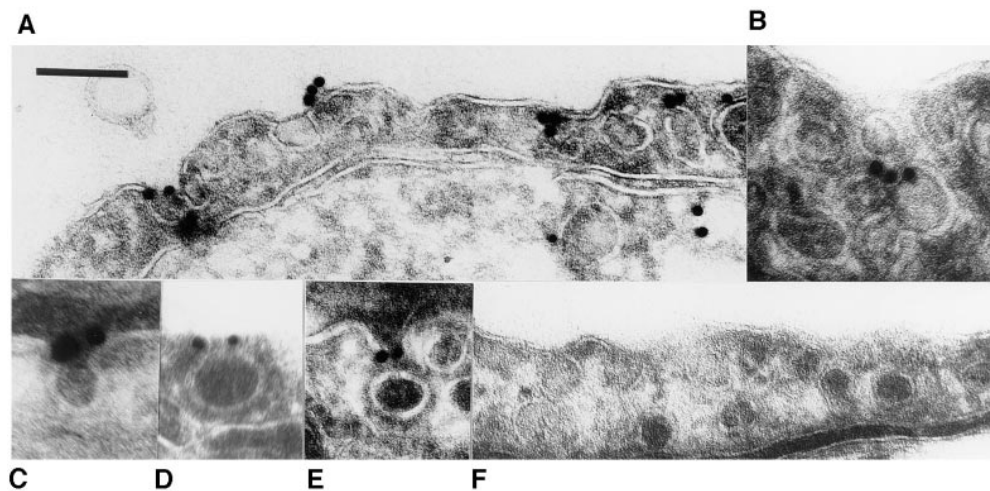


**Figure 13.** Dynamin localization to the neck of caveolae in endothelium in vivo. Immunogold electron microscopy (15-nm gold) was performed on ultrathin cryosections of rat lung tissue using antibody to dynamin (A–E) and control monoclonal antibody (F). Bar: (A, B, and D–F) 150 nm; (C) 72 nm.

lecular composition of the GTP-budded free caveolar vesicles called  $V_{\text{bud}}$  relative to the starting plasma membrane. Fig. 16 shows that just like caveolin, the caveolar markers  $G_{\text{M1}}$  and the TX3.833 antigen were present and quite enriched in  $V_{\text{bud}}$ , whereas 5'NT and  $\beta$ -actin were not. The free floating, low-density budded caveolae isolated on a continuous sucrose gradient were selectively rich in caveolar markers but not noncaveolar plasmalemma markers.

Lastly, we wondered whether dynamin, which is concentrated at the neck of caveolae and is rich in caveolae purified from the plasma membranes by physical disruption (remember we have shown the necks are intact in these isolated vesicles (Schnitzer et al., 1995c), would stay associated with the caveolae after they bud to form free caveolar vesicles. As shown in Fig. 16, dynamin was no longer associated with the caveolar vesicles after fission from the plasma membranes. Also note in Fig. 9 that in the presence of K44A cytosol where GTP-induced budding did not occur, dynamin was amply present on the plasma membrane whereas after GTP-induced budding in wild-type cytosol, the level of dynamin was greatly reduced. These results were quite consistent with dynamin binding around the neck of caveolae and requiring its ability to hydrolyze GTP to complete the fission process that releases vesicles rich in caveolar markers. Upon hydrolysis of GTP and the fission of caveolae, there was no need for dynamin to stay associ-

ated with the caveolae. It could then return to the cytosolic pool from whence it originally was drawn to the membrane.

### Discussion

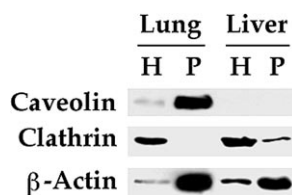
Dynamin is a putative mechanochemical GTPase with an interesting and yet curious ability to oligomerize around microtubules (Obar et al., 1990) and GTP $\gamma$ S-induced membrane tubules (Takei et al., 1995), as well as form oligomeric rings in low salt solution (Hinshaw and Schmid, 1995). Originally, because of dynamin's in vitro association with microtubules, it was thought to be a motor protein involved in microtubule-dependent cell motility (Obar et al., 1990). More recently, various studies have suggested a crucial regulatory role for dynamin in endocytosis. In *Drosophila*, temperature-sensitive mutants of the *shibire* gene, a homologue of the mammalian dynamin gene (Chen et al., 1991; Van der Bleik and Meyerowitz, 1991), manifest a pleotropic defect in vesicular budding from plasma membranes including: (a) the total abrogation of fluid phase or adsorptive endocytosis (Kosaka and Ikeda, 1983b; Masur et al., 1990); (b) the prevention of neuronal endocytic recycling of plasma membrane required for restoring synaptic vesicles after neurotransmission (Kosaka and Ikeda, 1983a) and avoiding the most striking defect of this mutant, paralysis (Poodry and Edgar, 1979; Van der Bleik and Meyerowitz, 1991); and (c) the accumulation of large numbers of clathrin-coated and non-clathrin-coated plasmalemmal invaginations as well as extended membrane tubules (Poodry and Edgar, 1979; Kosaka and Ikeda, 1983a,b; Kessel et al., 1989;

**Table II.** Analysis of Dynamin Localization in Endothelium by Immunogold Electron Microscopy

Dynamin	Endothelial Cell			Plasma Membrane		Caveolae	
	PM	Cytoplasm	ICM	Proper	Caveolae	Bulb	Neck
Gold	228	61	41	56	172	44	126
%	69.1	18.4	12.4	24.6	75.4	25.9	74.1

Ultrathin cryosections immunolabeled with the monoclonal antibody to dynamin were examined and photographed by electron microscopy (see Materials and Methods). Gold particles associated with the endothelium were counted. First, gold particles associated with the plasma membrane (PM) were distinguished from those apparently free in the cytoplasm and those associated with intracellular membranes (ICM). Next, on close examination of the plasma membrane, gold particles directly in association with plasma membrane but not associated with caveolae (Proper) were scored separately from those directly labeling caveolar membranes. Finally, gold particles clearly associated with the neck of caveolae were quantified separately from those labeling the rest of the caveolae, namely the bulb region.

**Figure 14.** Expression of clathrin and caveolin on endothelial cell plasma membranes isolated from rat lung and liver. Western analysis for caveolin,  $\beta$ -actin, and the heavy chain of clathrin was performed on tissue homogenates (H) and silica-coated endothelial cell plasma membranes (P) isolated from lung and liver.



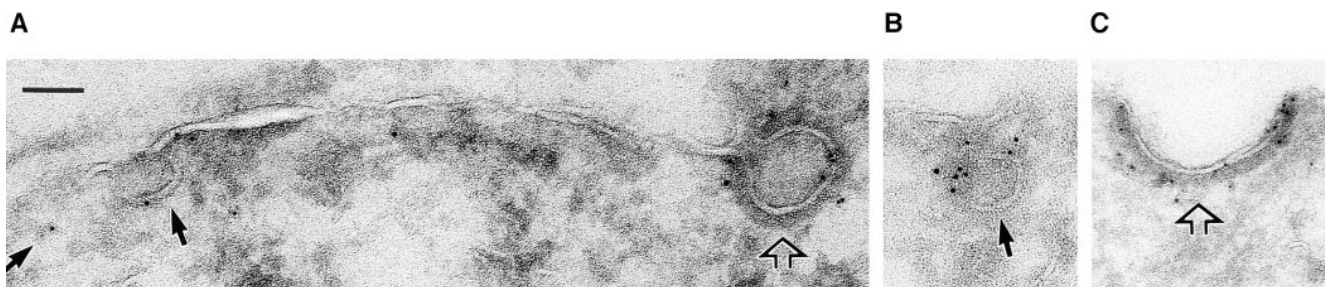


**Figure 15.** Dynamin labeling of caveolae and clathrin-coated pits in cultured endothelial cells. Immunogold labeling for dynamin (5-nm gold) was performed on ultrathin cryosections of cultured BAEC. (A) Labeled caveolae (*solid arrows*) (partial or forming caveola on left of fully formed caveolae) and clathrin-coated invagination (*open arrow*). (B) Single caveolae with gold label concentrated in the neck region. (C) Single clathrin-coated pit showing labeling over all areas of clathrin coat. Bar: (A and B) 76 nm; (C) 91 nm.

Koenig and Ikeda, 1989; Masur et al., 1990). Many of the same characteristics are observed in mammalian cells overexpressing dominant-negative mutants of dynamin (Herskovits et al., 1993; Van der Bleik et al., 1993; Damke et al., 1994, 1995*a,b*; Hinshaw and Schmid, 1995). The budding of clathrin-coated vesicles is blocked by mutants of dynamin (such as K44E or K44A) at a step clearly occurring after the formation of coated pits, possibly at the initial stages of receptor-mediated endocytosis (Herskovits et al., 1993), the wide-neck stage (Van der Bleik et al., 1993), or the formation of a “constricted” coated pit (Damke et al., 1994). Most recently, based on dynamin’s ability to form ringlike structures in solution (Hinshaw and Schmid, 1995) and GTP $\gamma$ S-induced membrane tubules (Takei et al., 1995), it was speculated that dynamin affects even a later step in the budding process involving fission at the neck of the forming invagination. Thus, although dynamin clearly plays an important role in endocytosis, how and where dynamin has its effect in the budding process has been rather uncertain.

Here, for the first time, our results provide direct information not only about dynamin’s immediate role in the fission step of the budding of plasmalemmal vesicles to form free transport vesicles, but also its function in the budding of a different type of plasmalemmal invagination independent of clathrin, namely caveolae. In the reconstituted cell-free assay used here, only the last step in caveolar budding, namely fission, can be examined because the plasma membranes have been coated during purification with colloidal silica particles that are too large to penetrate the introit at the neck and therefore do not enter the fully

	P	V <sub>bud</sub>	V <sub>bud</sub> /P
Caveolin			15
TX3.833			23
GM <sub>1</sub>			7
5'NT			0.03
Dynamin			0.04
$\beta$ -Actin			0.06

**Figure 16.** GTP-budded free caveolar vesicles contain specific caveolar markers but lack dynamin. Western analysis with antibodies to the indicated proteins was performed on P (before the budding reaction) and V<sub>bud</sub> the caveolar vesicles induced to bud by GTP in wild-type dynamin cytosol and isolated by flotation in a continuous sucrose gradient. The signal was quantified densitometrically and the ratio of V<sub>bud</sub>/P is provided as an indication of enrichment under equal protein loads (2  $\mu$ g).

formed, flask-shaped caveolae. By remaining firmly and uniformly attached to the other regions of the plasma membrane, this coating prevents the de novo formation of invaginations but allows the completion of the budding process through GTP-dependent fission of the already formed caveolar invaginations (Schnitzer et al., 1996). Unlike clathrin-coated invaginations, caveolae exist predominantly in a mature fully formed shape with a well-developed neck and bulb region. By using this assay, we demonstrate that dynamin’s specific role in budding must indeed be at or very near the final fission step releasing the carrier vesicle from the plasma membrane.

From our findings, it is very unlikely that dynamin’s function in budding and endocytosis is exclusive for clathrin-coated vesicles as recently suggested by some (Damke et al., 1995*a*) but not other (Artalejo et al., 1995; Shpetner et al., 1996) findings. Potentially consistent with this role for dynamin, fluid phase pinocytosis is blocked in various cells from the shibire flies (Kosaka and Ikeda, 1983*b*; Masur et al., 1990). Unlike the shibire cells, transfected HeLa cells appear able to compensate for mutant dynamin expression to allow the penetration and apparent intracellular accumulation of fluid phase probes, possibly by a dynamin- and/or clathrin-independent engulfing mechanism that as yet remains obscure (Damke et al., 1994, 1995*a,b*). In contrast, immunofluorescence studies on Cos cells show dynamin binding to clathrin-coated as well as non-clathrin-coated cell surface regions, with the latter so far being undefined (Shpetner et al., 1996). A recent functional study (Artalejo et al., 1995) shows that in secretory adrenal chromaffin cells, the rapid endocytic recapture of exocytic vesicle membranes normally occurring after stimulated secretion was dependent on GTP hydrolysis and dynamin but apparently not clathrin. Interestingly, by Western analysis, we detect caveolin in Cos cells but not HeLa cells (our unpublished observations). Various types of noncoated plasmalemmal vesicles are likely to exist and as yet, each type has not been distinguished biochemically with its own marker proteins. Here, we establish for the first time dynamin’s direct association with one type of clathrin-independent plasmalemmal vesicle, namely caveolae, and have demonstrated its direct role in their fission from the plasma membrane.

It is attractive to speculate that dynamin is assembled around the necks of plasmalemmal invaginations to permit vesicle fission with GTP hydrolysis. Although various models describing dynamin’s role in budding have placed

it at the neck of budding clathrin-coated invaginations (Hinshaw and Schmid, 1995; Takei et al., 1995), direct evidence for its existence *in vivo* at this presumed site of action has surprisingly been lacking, especially under normal, unperturbed conditions. In HeLa cells, dynamin has been localized rather diffusely over both clathrin-coated pits without any preference for the neck region and small flat plasmalemmal regions of an undefined nature (Damke et al., 1994). Here, we show for the first time that dynamin does indeed exist at its logical site of action, in this case the neck of caveolae, where it has been shown to be effective in caveolar fission. At least for caveolae in endothelium, one need not postulate that dynamin rings around the necks of plasmalemmal vesicles are extremely transient structures, which may require GTP $\gamma$ S arrest and polymeric ring extension to be detected.

There may be other differences between caveolae and clathrin-coated vesicles with regards to dynamin and its mechanism of action. The rather significant enrichment of dynamin in the purified caveolae that we observed (Fig. 11) may be remarkable because dynamin has been reported to be present but not concentrated in purified clathrin-coated vesicles (Takei et al., 1995). They contain less dynamin per unit protein than the total starting homogenate whereas caveolae in endothelium have a 30–40-fold enrichment in dynamin ( $V$  relative to  $H$  in Fig. 11 *A*). This difference may reflect on the type of clathrin-coated vesicle isolated that, at least from the rat brain, may include both budded free clathrin-coated vesicles and clathrin-coated vesicles physically separated from the membranes by homogenization. In our study, we found that caveolae that have budded away from the plasma membrane lacked dynamin, whereas those physically separated from the plasma membrane (with their necks intact) were quite enriched in dynamin. Thus, the trivial explanation for this difference may be that the isolated brain clathrin vesicles consist primarily of the budded variety and not those torn away from the plasma membrane. One concern in this regard may be that during clathrin-mediated endocytosis it is believed that the clathrin is released from the budded vesicle rather quickly, to apparently allow fusion with target membranes. Although more work is necessary to clarify these differences, in the end these potential differences between caveolae and clathrin-coated vesicles may simply reflect on distinctive budding mechanisms. Dynamin as a cytosolic protein may be present rather transiently on the neck of clathrin-coated invaginations in a stage-dependent manner. Conversely, caveolae may require dynamin first to stabilize their necks to create and maintain their most commonly seen, fully formed shape, and then later to become activated for fission by specific signaling events as yet undefined. Could caveolae be poised or primed awaiting a key signal to initiate rapid fission?

Dynamin may join caveolin as the second identified structural protein of caveolae. We have found that caveolar dynamin is solubilized by Triton X-100 even at 4°C (our unpublished observations), which required us to purify caveolae in the absence of any detergent and may explain why caveolae, that are by nature resistant to detergent solubilization, can be sheared away from plasma membranes more easily after Triton X-100 treatment (Schnitzer et al., 1995c). As a protein known to form oligo-

meric rings in solution (Hinshaw and Schmid, 1995), to polymerize on lipid membranes (Tuma and Collins, 1995), and to form helical twists surrounding thin membrane tubes induced by GTP $\gamma$ S (Takei et al., 1995), dynamin is likely to provide a critical stabilizing ‘collar’ at the shearing breakpoint, which is at the caveolar neck (Schnitzer et al., 1996). Consistent with dynamin’s additional function as mediator of caveolar fission, caveolae purified after GTP-stimulated budding actually lack dynamin (Fig. 16). With its apparent dual functionality, it appears logical that dynamin be present around the neck of caveolae when they are attached to the plasma membrane but lost after the caveolae bud to form free transport vesicles.

### *A Model for Dynamin-mediated Fission and Future Work*

It is becoming clear that dynamin mediates the internalization of caveolae through a GTP-dependent fission process requiring its presence at the neck of caveolae and its ability to hydrolyze GTP. Purified dynamin exists as a tetramer that can spontaneously self-assemble in solution into rings  $\sim$ 10–20-nm wide and  $\sim$ 20–40-nm long as well as helical stacks of rings (Hinshaw and Schmid, 1995). In the presence of GTP $\gamma$ S, dynamin can form tubular invaginations with extended neck regions 25-nm wide (Takei et al., 1995). These dimensions fit nicely with those of the caveolar neck and are consistent with our detection of dynamin at the neck of caveolae.

Based on this and other currently available data, we propose the following mechanistic model. In a manner analogous to its formation of oligomeric rings (Hinshaw and Schmid, 1995), membrane tubules with extended necks (Takei et al., 1995) and probably “collared” plasmalemmal vesicles in *shibire* flies (Kosaka and Ikeda, 1983a), dynamin, either in its unoccupied or GDP-bound form, is likely to bind and polymerize to form a stabilizing “collar” around the neck of the caveola, possibly through a process facilitated by the interaction of its basic COOH-terminal domain with membrane lipids (Tuma et al., 1993). This collar may be structurally important for the formation of mature flask-shaped caveolae with a clear neck and bulb region. To mediate fission, the dynamin in this oligomeric collar must become activated to increase its ability to bind and hydrolyze GTP to a critical level permitting fission. This process may occur in part through the direct effects of anionic lipids (Tuma and Collins, 1995) such as phosphoinositides (Lin and Gilman, 1996), which do exist in caveolae (Liu et al., 1997) and may require specific signaling events for their production or metabolism to more potent, activating forms. Such effectors may even cause additional dynamin to bind, thereby potentiating even further the GTPase activity of the growing oligomer (Tuma and Collins, 1994). Upon attainment of the critical GTPase activity level, dynamin’s hydrolysis of GTP supplies enough energy to drive “constriction” via conformational changes in the dynamin oligomer which provide the “pinching” force necessary for bringing the invaginated membranes at the neck in close enough apposition to permit membrane fusion and thus vesicle fission. Upon culmination of this process, dynamin appears to be completely released from the caveolae to the cytosol and the caveolae bud to become in-

ternalized free carrier vesicles capable of moving their molecular cargo to intracellular or transcellular destinations. Future work needs to focus on the mechanism(s) and chronology of the cascade that increase dynamin's GTPase activity to the level critical for severing nascent invaginations.

We thank T. Horner and M. Ericsson for technical assistance and advice; K. Baker for the early passage BAEC; S. Schmid and D. Warnock for the generous gift of the transfected HeLa cells and purified dynamins; and R. Vallee and colleagues for the wild-type and K44E mutant dynamin DNA subcloned into pSVL.

This work was supported in part by National Institutes of Health grants HL52766 and HL58216 (to J.E. Schnitzer) and a Grant-in-Aid from the American Heart Association (to J.E. Schnitzer). J.E. Schnitzer is supported in part by an Established Investigator Award from American Heart Association and Genentech.

Received for publication 20 May 1997 and in revised form 27 January 1998.

*Note Added in Proof.* Another laboratory, using a different experimental system and cell type, has confirmed a role for dynamin in caveolar internalization (see accompanying paper by Henley, J.R., E.W.A. Krueger, B.J. Oswald, and M.A. McNiven. 1998. *J. Cell Biol.* 141:85–99).

## References

- Anderson, R.G. 1993. Caveolae: where incoming and outgoing messengers meet. *Proc. Natl. Acad. Sci. USA.* 90:10909–10913.
- Artalejo, C.R., J.R. Henley, M.A. McNiven, and H.C. Palfrey. 1995. Rapid endocytosis coupled to exocytosis in adrenal chromaffin cells involves  $Ca^{2+}$ , GTP and dynamin but not clathrin. *Proc. Natl. Acad. Sci. USA.* 92:8328–8332.
- Chen, M.S., R.A. Obar, C.C. Schroeder, T.W. Austin, C.A. Poodry, S.C. Wadsworth, and R.B. Vallee. 1991. Multiple forms of dynamin are encoded by shibire, a *Drosophila* gene involved in endocytosis. *Nature.* 351:583–586.
- Damke, H., T. Baba, D.E. Warnock, and S.L. Schmid. 1994. Induction of mutant dynamin specifically blocks endocytic coated vesicle formation. *J. Cell Biol.* 127:915–934.
- Damke, H., T. Baba, A.M. van der Blik, and S.L. Schmid. 1995a. Clathrin-independent pinocytosis is induced in cells overexpressing a temperature-sensitive mutant of dynamin. *J. Cell Biol.* 131:69–80.
- Damke, H., M. Gossen, S. Freundlieb, H. Bujard, and S.L. Schmid. 1995b. Tightly regulated and inducible expression of dominant interfering dynamin mutant in stably transformed HeLa cells. *Methods Enzymol.* 257:209–220.
- Fra, A.M., E. Williamson, K. Simons, and R.G. Parton. 1995. De novo formation of caveolae in lymphocytes by expression of VIP21-caveolin. *Proc. Natl. Acad. Sci. USA.* 92:8655–8659.
- Ghitescu, L., A. Fixman, M. Simionescu, and N. Simionescu. 1986. Specific binding sites for albumin restricted to plasmalemmal vesicles of continuous capillary endothelium: Receptor-mediated transcytosis. *J. Cell Biol.* 102:1304–1311.
- Griffiths, G. 1993. *Fine Structure Immunocytochemistry.* Heidelberg, Springer Verlag. 237–278.
- Herskovits, J.S., C.C. Burgess, R.A. Obar, and R.B. Vallee. 1993. Effects of mutant rat dynamin on endocytosis. *J. Cell Biol.* 122:565–578.
- Hinshaw, J.E., and S.L. Schmid. 1995. Dynamin self-assembles into rings suggesting a mechanism for coated vesicle budding. *Nature.* 374:190–192.
- Kartenback, J., H. Stuckenbrock, and A. Helenius. 1989. Endocytosis of simian virus 40 into the endoplasmic reticulum. *J. Cell Biol.* 109:2721–2729.
- Kessel, I., B.D. Holst, and T.F. Roth. 1989. Membranous intermediates in endocytosis are labile, as shown in a temperature-sensitive mutant. *Proc. Natl. Acad. Sci. USA.* 86:4968–4972.
- Koenig, J.H., and K. Ikeda. 1989. Disappearance and reformation of synaptic vesicle membrane upon transmitter release observed under reversible blockage of membrane retrieval. *J. Neurosci.* 9:3844–3860.
- Kosaka, T., and K. Ikeda. 1983a. Possible temperature-dependent blockage of synaptic vesicle recycling induced by a single gene mutation in *Drosophila*. *J. Neurobiol.* 14:207–225.
- Kosaka, T., and K. Ikeda. 1983b. Reversible blockade of membrane retrieval and endocytosis in the garland cell of the temperature-sensitive mutant of *Drosophila melanogaster*, shibire. *J. Cell Biol.* 97:499–507.
- Li, S., J. Couet, and M.P. Lisanti. 1996. Src tyrosine kinase,  $G\alpha$  subunits, and H-Ras share a common membrane-anchored scaffolding protein, caveolin. Caveolin binding negatively regulates the auto-activation of Src tyrosine kinases. *J. Biol. Chem.* 271:29182–29190.
- Lin, H.C., and A.G. Gilman. 1996. Regulation of dynamin I GTPase activity by G protein  $\beta\gamma$  subunits and phosphatidylinositol 4,5-bisphosphate. *J. Biol. Chem.* 271:27979–27982.
- Lisanti, M.P., P.E. Scherer, Z. Tang, and M. Sargiacomo. 1994. Caveolae, caveolin and caveolin-rich membrane domains: a signalling hypothesis. *Trends Cell Biol.* 4:231–235.
- Liu, J., P. Oh, T. Horner, R.A. Rogers, and J. Schnitzer. 1997. Organized endothelial cell surface signal transduction in caveolae distinct from glycosylphosphatidyl-anchored protein microdomains. *J. Biol. Chem.* 272:7211–7222.
- Masur, S.K., Y. Kim, and C. Wu. 1990. Reversible inhibition of endocytosis in cultured neurons from the *Drosophila* temperature-sensitive mutant shibire. *J. Neurogenetics.* 6:191–206.
- Milici, A.J., N.E. Watrous, H. Stukenbrok, and G.E. Palade. 1987. Transcytosis of albumin in capillary endothelium. *J. Cell Biol.* 105:2603–2612.
- Monier, S., R.G. Parton, F. Vogel, J. Behlke, A. Henske, and T.V. Kurzchalia. 1995. VIP21-caveolin, a membrane protein constituent of the caveolar coat, oligomerizes *in vivo* and *in vitro*. *Mol. Biol. Cell.* 6:911–927.
- Montesano, R., J. Roth, A. Robert, and L. Orci. 1982. Non-coated membrane invaginations are involved in binding and internalization of cholera and tetanus toxins. *Nature.* 296:651–653.
- Obar, R.A., C.A. Collins, J.A. Hammarback, H.S. Shpetner, and R.B. Vallee. 1990. Molecular cloning of the microtubule-associated mechanochemical enzyme dynamin reveals homology with a new family of GTP-binding proteins. *Nature.* 347:256–261.
- Palade, G.E. 1958. Transport in quanta across the endothelium of blood capillaries. *Anat. Rec.* 130:467.
- Parton, R.G. 1994. Ultrastructural localization of gangliosides;  $GM_1$  is concentrated in caveolae. *J. Histochem. Cytochem.* 42:155–166.
- Poodry, C.A., and L. Edgar. 1979. Reversible alterations in the neuromuscular junctions of *Drosophila melanogaster* bearing a temperature-sensitive mutation, shibire. *J. Cell Biol.* 81:520–527.
- Rothberg, K.G., J.E. Heuser, W.C. Donzell, Y.S. Ying, J.R. Glenney, and R.G. Anderson. 1992. Caveolin, a protein component of caveolae membrane coats. *Cell.* 68:673–682.
- Sargiacomo, M., P.E. Scherer, Z. Tang, E. Kubler, K.S. Song, M.C. Sanders, and M.P. Lisanti. 1995. Oligomeric structure of caveolin: implications for caveolae membrane organization. *Proc. Natl. Acad. Sci. USA.* 92:9407–9411.
- Schnitzer, J.E. 1993. Update on the cellular and molecular basis of capillary permeability. *Trends Cardiovasc. Med.* 3:124–130.
- Schnitzer, J.E. 1997. The endothelial cell surface and caveolae in health and disease. In *Vascular Endothelium: Physiology, Pathology and Therapeutic Opportunities.* G.V.R. Born, and C.J. Schwartz, editors. Schattauer, Stuttgart, Germany. 77–95.
- Schnitzer, J.E., and J. Bravo. 1993. High affinity binding, endocytosis and degradation of conformationally-modified albumins: potential role of gp30 and gp18 as novel scavenger receptors. *J. Biol. Chem.* 268:7562–7570.
- Schnitzer, J.E., and P. Oh. 1994. Albondin-mediated capillary permeability to albumin: differential role of receptors in endothelial transcytosis and endocytosis of native and modified albumins. *J. Biol. Chem.* 269:6072–6082.
- Schnitzer, J.E., P. Oh, E. Pinney, and J. Allard. 1994. Filipin-sensitive caveolae-mediated transport in endothelium: Reduced transcytosis, scavenger endocytosis, and capillary permeability of select macromolecules. *J. Cell Biol.* 127:1217–1232.
- Schnitzer, J.E., J. Allard, and P. Oh. 1995a. NEM inhibits transcytosis, endocytosis, and capillary permeability: implication of caveolae fusion in endothelium. *Am. J. Physiol.* 268:48–55.
- Schnitzer, J.E., J. Liu, and P. Oh. 1995b. Endothelial caveolae have the molecular transport machinery for vesicle budding, docking, and fusion including VAMP, NSF, SNAP, annexins, and GTPases. *J. Biol. Chem.* 270:14399–14404.
- Schnitzer, J.E., P. Oh, A.M. Dvorak, J. Liu, and D.P. McIntosh. 1995c. Separation of caveolae from associated microdomains of GPI-anchored proteins. *Science.* 269:1435–1439.
- Schnitzer, J.E., P. Oh, B.S. Jacobson, and A.M. Dvorak. 1995d. Caveolae from luminal plasmalemma of rat lung endothelium: microdomains enriched in caveolin,  $Ca^{2+}$ -ATPase, and inositol triphosphate receptor. *Proc. Natl. Acad. Sci. USA.* 92:1759–1763.
- Schnitzer, J.E., P. Oh, and D.P. McIntosh. 1996. Role of GTP hydrolysis in fission of caveolae directly from plasma membranes. [published erratum appears in *Science.* 1996. 274:1069]. *Science.* 274:239–242.
- Shpetner, H.S., J.S. Herskovits, and R.B. Vallee. 1996. A binding site for SH3 domains targets dynamin to coated pits. *J. Biol. Chem.* 271:13–16.
- Takei, K., P.S. McPherson, S.L. Schmid, and P. De Camilli. 1995. Tubular membrane invaginations coated by dynamin rings are induced by GTP- $\gamma$ S in nerve terminals. *Nature.* 374:186–192.
- Tuma, P.L., and C.A. Collins. 1994. Activation of dynamin GTPase is a result of positive cooperativity. *J. Biol. Chem.* 269:30842–30847.
- Tuma, P.L., and C.A. Collins. 1995. Dynamin forms polymeric complexes in the presence of lipid vesicles. *J. Biol. Chem.* 270:26707–26714.
- Tuma, P.L., M.C. Stachniak, and C.A. Collins. 1993. Activation of dynamin GTPase by acidic phospholipids and endogenous rat brain vesicles. *J. Biol. Chem.* 268:17240–17246.
- Van der Bleik, A.M., and E.M. Meyerowitz. 1991. Dynamin-like protein encoded by the *Drosophila* shibire gene associated with vesicular traffic. *Nature.* 351:411–414.
- Van der Bleik, A.M., T.E. Redelmeier, H. Damke, E.J. Tisdale, E.M. Meyerowitz, and S.L. Schmid. 1993. Mutations in human dynamin block an intermediate stage in coated vesicle formation. *J. Cell Biol.* 122:553–563.